

## Critical micelle concentration from a lattice gas model

This article has been downloaded from IOPscience. Please scroll down to see the full text article.

1989 J. Phys.: Condens. Matter 1 4245

(<http://iopscience.iop.org/0953-8984/1/26/018>)

View [the table of contents for this issue](#), or go to the [journal homepage](#) for more

Download details:

IP Address: 171.66.16.93

The article was downloaded on 10/05/2010 at 18:23

Please note that [terms and conditions apply](#).

## LETTER TO THE EDITOR

# Critical micelle concentration from a lattice gas model

W Wenzel<sup>†</sup>, C Ebner<sup>†</sup>, C Jayaprakash<sup>†</sup> and Rahul Pandit<sup>‡</sup>

<sup>†</sup> Department of Physics, Ohio State University, Columbus, Ohio 43210, USA

<sup>‡</sup> Department of Physics, Indian Institute of Science, Bangalore 560012, India

Received 23 March 1989

**Abstract.** The temperature dependence of the critical micelle concentration (CMC) and a closed-loop coexistence curve are obtained, via Monte Carlo simulations, in the water-surfactant limit of a two-dimensional version of a statistical mechanical model for microemulsions. The CMC and the coexistence curve reproduce various experimental trends as functions of the couplings. In the oil-surfactant limit, there is a conventional coexistence curve with an upper consolute point that allows for a region of three-phase coexistence between oil-rich, water-rich and microemulsion phases.

Binary mixtures of water and surfactant molecules often exhibit (1) a ‘critical micelle concentration’ (CMC) [1, 2] of surfactants at which these molecules form large aggregates called micelles, and (2) a closed-loop coexistence curve [1, 3] in the  $n_s$ - $T$  phase diagram;  $n_s$  is the density of surfactant molecules. If, in addition, oil is added to the water-surfactant mixture, a variety of phases, including microemulsions, and phase equilibria can be obtained.

In this Letter we propose a lattice model for oil-water-surfactant mixtures [4]. We have studied our model in two dimensions using Monte Carlo (MC) simulations. Our principal results are as follows. (1) In a range of physically admissible parameters, we find a CMC in the water-surfactant limit; the temperature dependence of the CMC is in agreement with experiments (figure 1). This is, to our knowledge, the first detailed lattice gas calculation that yields a CMC that has reasonable dependence on various parameters. (2) Within the same range of parameters, our model has a closed-loop coexistence curve (figure 1) in the water-surfactant limit, with a lower consolute point, called the cloud point, at a temperature  $T_\alpha$ . (3) In the oil-surfactant limit, our model yields a conventional coexistence curve with an upper consolute point at a temperature  $T_\beta$ . (4) Within this range of parameters  $T_\alpha$  may be greater than  $T_\beta$ ; thus we may conclude that our model can exhibit three-phase coexistence between oil-rich, water-rich and microemulsion phases.

Our model is defined on a  $d$ -dimensional hyper-cubic lattice (with sublattices A and B). It has site variables  $\sigma_i$  which can assume values 1, 0, and  $-1$ , depending, respectively, on whether a water molecule, a vacancy, or an oil molecule occupies site  $i$ . Vacancies at sites allow for excluded-volume effects or steric constraints in an approximate fashion while still permitting extensive numerical simulations. There are also link variables  $\tau_{ij}$  with values 1, 0,  $-1$ ; 0 denotes the absence of a surfactant molecule on link  $ij$ , whereas  $1(-1)$  denotes the presence of a surfactant molecule with its head pointing towards the

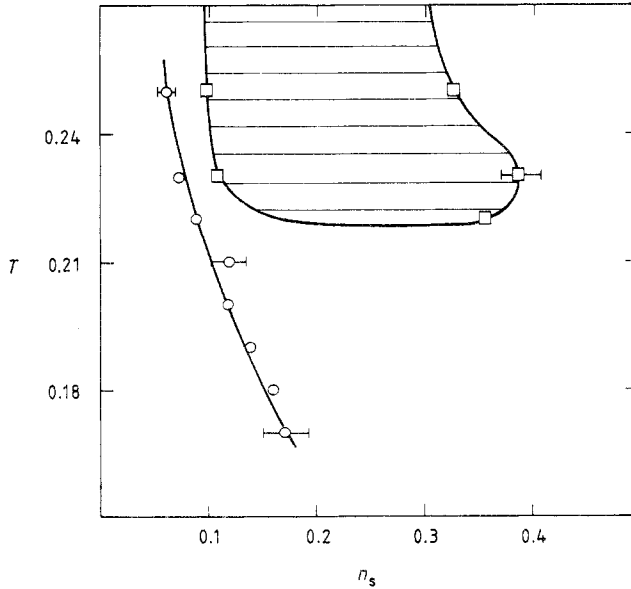


**Figure 1.** Monte Carlo phase diagram in the temperature (in units of  $J$ ),  $n_s$  plane. The coexistence curve is indicated by squares, the CMC by open circles. The lines are included to guide the eye. The two-phase region is hatched by tie lines. Parameter values for this figure are:  $D = -0.95$ ,  $B_{12} = 1.0$ ,  $B_{34} = -0.3$ ,  $V_1 = 0$ ,  $V_2 = 0.1$ . Representative error bars are given.

site on sublattice A (B), thus incorporating the directionality of the surfactant molecule. The Hamiltonian is

$$\begin{aligned}
 \mathcal{H} = & H \sum_i \sigma_i - J \sum_{\langle ij \rangle} \sigma_i \sigma_j - \Delta \sum_i \sigma_i^2 - \mu \sum_{\langle ij \rangle} \tau_{ij}^2 \\
 & - B_1 \sum'_{\langle ij \rangle} \tau_{ij} (\sigma_i - \sigma_j) - B_2 \sum'_{\langle ij \rangle} \tau_{ij} (\sigma_i^2 - \sigma_j^2) - B_3 \sum_{\langle ij \rangle} \tau_{ij}^2 (\sigma_i + \sigma_j) \\
 & - B_4 \sum_{\langle ij \rangle} \tau_{ij}^2 (\sigma_i^2 + \sigma_j^2) - V_1 \sum'_{\langle ij, ik \rangle} (\tau_{ij} \tau_{ik}^2 + \tau_{ij}^2 \tau_{ik}) - V_2 \sum_{\langle ij, ik \rangle} \tau_{ij}^2 \tau_{ik}^2 \quad (1)
 \end{aligned}$$

where  $\langle ij \rangle$  denotes nearest-neighbour pairs of sites and  $\langle ij, ik \rangle$ , nearest-neighbour pairs of links. In the primed sums, if site  $i$  is in sublattice A (B), a positive (negative) sign is associated with the summand. The parameters  $H$  and  $\Delta$  play the role of chemical potentials for the oil and water;  $\mu$  is the chemical potential for the surfactant molecules. The bare oil–water interaction is  $J \equiv 1$ , producing phase separation of oil and water in the absence of surfactants. The parameters  $B_k$ ,  $k = 1, 2, 3, 4$ , control the hydrophilicity and hydrophobicity of the surfactants and their relative solubility in oil and water. Finally,  $V_1$  and  $V_2$  approximately account for interactions between surfactant molecules. We pick them so that heads (tails) repel (attract) each other. The parameters are restricted substantially if we demand that the phase diagram of the model display various experimental features in the water–surfactant or oil–surfactant limit.

To obtain the water–surfactant limit, let  $H \rightarrow \infty$  and  $\Delta \rightarrow -\infty$ , with  $H + \Delta = 2D$ ,  $D$  finite. Then  $S_i \equiv (2\sigma_i - 1)$  can only assume the values  $+1$  ( $-1$ ) representing water (vacancies), and  $\mathcal{H}$  is

$$\begin{aligned} \mathcal{H} = & -(D + J) \sum_i S_i - \frac{J}{4} \sum_{\langle ij \rangle} S_i S_j - B_{12} \sum_{\langle ij \rangle}' \tau_{ij} (S_i - S_j) \\ & - B_{34} \sum_{\langle ij \rangle} \tau_{ij}^2 (S_i + S_j) - (\mu + 2B_{34}) \sum_{\langle ij \rangle} \tau_{ij}^2 \\ & - V_1 \sum_{\langle ij, ik \rangle}' (\tau_{ij} \tau_{ik}^2 + \tau_{ij}^2 \tau_{ik}) - V_2 \sum_{\langle ij, ik \rangle} \tau_{ij}^2 \tau_{ik}^2 \end{aligned} \quad (2)$$

where  $B_{mn} \equiv (B_m + B_n)/2$ ,  $m, n = 1, 2$  or  $3, 4$ . The oil–surfactant limit may be obtained similarly.

We discuss first the case  $V_1 = V_2 = 0$ , for which, in the evaluation of the partition function, the trace over  $\tau_{ij}$  can be performed trivially to give an effective Ising model with an exchange coupling (in two dimensions)

$$\begin{aligned} J_{\text{eff}}(T, \mu) = & (J/4) + (k_B T/4) \ln \{ [1 + 2 \exp(\beta\mu)] \{ 1 + \exp[\beta(\mu + 2B_{34})] \} \\ & \times \{ 1 + 2 \exp[\beta(\mu + 2B_{34})] \cosh(\beta B_{12}) \}^{-1} \} \end{aligned} \quad (3)$$

and a magnetic field

$$H_{\text{eff}}(T, \mu) = D + J - k_B T \ln \{ [1 + 2 \exp(\beta\mu)] \{ 1 + 2 \exp[\beta(\mu + 2B_{34})] \} \}. \quad (4)$$

This model has a critical point whenever  $H_{\text{eff}} = 0$  and  $\beta J_{\text{eff}} = -[\ln(2^{1/2} - 1)]/2$ . Thus we can find the phase diagram in the  $T - \mu$  or  $T - n_s$  planes. We obtain a closed-loop coexistence curve, via the mechanism noted previously [5] (and references therein), in the  $T - n_s$  plane in certain ranges of parameters; e.g., it is obtained with  $-1 < D < -0.7$ ,  $B_{34} < 0$ , and  $|B_{34}| < B_{12} < 2|B_{34}|$ .

The dependence of the shape and position of the coexistence curve on parameters is in qualitative accord with experiments. Increasing  $B_{12}$  corresponds to increasing the hydrophobicity of surfactant molecules. This decreases the size of the loop both in our model and in experimental systems [1, 3]. The loop can be moved parallel to the  $n_s$  axis by changing  $B_{34}$ , which controls the solubility of surfactant molecules (a large value of  $B_{34}$  leads to a large solubility). Also, near the cloud point the coexistence curve in our model is flat, as in experimental water–surfactant mixtures.

Given  $V_1$  and  $V_2$  non-zero, we obtain the phase diagram of model (2) from MC simulations. The closed loop persists in certain ranges of parameters; e.g., we obtain it for  $1 < B_{12} < 0.6$ ,  $-0.5 < B_{34} < -0.1$ ,  $-0.95 < D < -0.7$ ,  $-0.05 < V_1 < 0$ , and  $0 < V_2$ . As  $V_1$  becomes large and negative, the heads of surfactant molecules repel each other strongly, causing  $T_\alpha$  to rise until, for  $V_1 < -0.1$ , it disappears completely. Large values of  $V_2$  lead to large overall attraction between surfactant molecules. It is not surprising therefore that increasing  $V_2$  shifts the left boundary of the coexistence curve to low values of  $n_s$ . Also for non-zero  $V_1$  and  $V_2$ , our model yields various trends for the coexistence curve (see the discussion above for  $V_1 = V_2 = 0$ ) that are in qualitative agreement with experiments.

Our model (2) also exhibits the phenomenon of micellisation, in which the surfactant molecules start to form large aggregates called micelles; we interpret as a micelle a connected cluster of vacancies, immersed in water and surrounded by a boundary layer

of surfactants. The vacancies represent in a rough way the exclusion of water from the micelle core, i.e., the region occupied by the hydrocarbon tails of the surfactants. The aggregates are compact, rapidly fluctuating structures, circular on average (and presumably spherical in three dimensions), with very little water penetration into the micellar core. Also, the number of enclosed vacancies is small for aggregates of up to 40 surfactant molecules. The shape of a micelle fluctuates rapidly, but the micelle retains its identity for on the order of 1000 Monte Carlo steps per spin (MCS). The constraints of the lattice introduce particular small clusters (for example a four-micelle, that is, four surfactants surrounding one vacancy), which we consider artifacts of the model, i.e. they are not considered to be micelles.

In our model, as in experiments [2], the onset of micellisation, i.e. the formation of large aggregates as a function of  $n_s$ , occurs abruptly at the CMC. This sudden change is not a true phase transition; it is conveniently pictured as an arrested phase separation [6]. To the best of our knowledge, our calculation is the first one for a lattice model which shows the variation of the CMC with  $T$  (the dashed line in figure 1) in qualitative agreement with experiments [2]. Other theoretical treatments of micellar solutions based on more phenomenological approaches exist [7]. The CMC falls with increasing hydrophobicity of the tail group of the surfactants. And, of course, since an increase in  $V_1$  increases the repulsion between the heads of surfactants, it hinders micellisation. Just above the CMC, the water–surfactant system is a dilute suspension of poly-disperse micelles, with the mean aggregation number increasing beyond the CMC. All of these features are in qualitative accord with experimental results.

Experimentally, the CMC is obtained by a variety of methods, such as surface tension, dye solubilisation and tautomer measurements [1, 2], to name a few. Without the introduction of yet another species, these cannot be realised within our model. We therefore computed the inverse osmotic compressibility  $\partial\pi/\partial n_s$  ( $\pi$  is the osmotic pressure) against  $n_s$  (figure 2(a)), finding a maximum at the CMC, as is to be expected if we think of micellisation at the CMC as an arrested phase separation [6]. The osmotic pressure has been used in experiments [8] to determine the CMC; we found it convenient (for numerical reasons) to employ the osmotic compressibility, which we find from the relation [9]  $(\partial\pi/\partial n_s)_{T,\mu_w} = k_B T \langle n_s \rangle / (\langle n_s^2 \rangle - \langle n_s \rangle^2)$ ;  $\mu_w$  is the chemical potential of water. As an independent check, we plot the numbers of small clusters (up to four surfactant molecules per cluster) and large micelles (more than four surfactant molecules per cluster) against the surfactant concentration  $n_s$  (figure 2(b)). The point at which the asymptotes to the ends of these curves meet yields the CMC. The saturation of the number of small clusters (figure 2(b)) for  $n_s > \text{CMC}$  is precisely what is expected on phenomenological grounds. All of the methods we use yield values for the CMC in our model that are within a few per cent of each other, although considerably larger than experimental values which are typically  $10^{-5} \text{ mol l}^{-1}$ . The lowest CMC we were able to observe was approximately at  $n_s = 0.02$ ; there was no indication that the effect would not persist in our model at even lower concentrations. In order to obtain good statistics on the aggregation, we chose the parameter values such that a sufficient number of surfactants is present in the system (for the results presented here).

At some temperatures the CMC occurs near the closed-loop coexistence curve, where fluctuations in  $n_s$  can be large. Therefore, the simulations have to be done very carefully. Our results using  $30^2$  and  $50^2$  lattices agree, indicating finite-size corrections are unimportant; in some cases we use  $70^2$  and  $100^2$  lattices to be sure. We equilibrate for up to 15000 MCS and then average over as many as 90000 MCS.

As described earlier, we have to restrict  $B_{12}$  and  $B_{34}$  to obtain the closed-loop phase diagram in the water–surfactant limit. There is still sufficient freedom to vary the

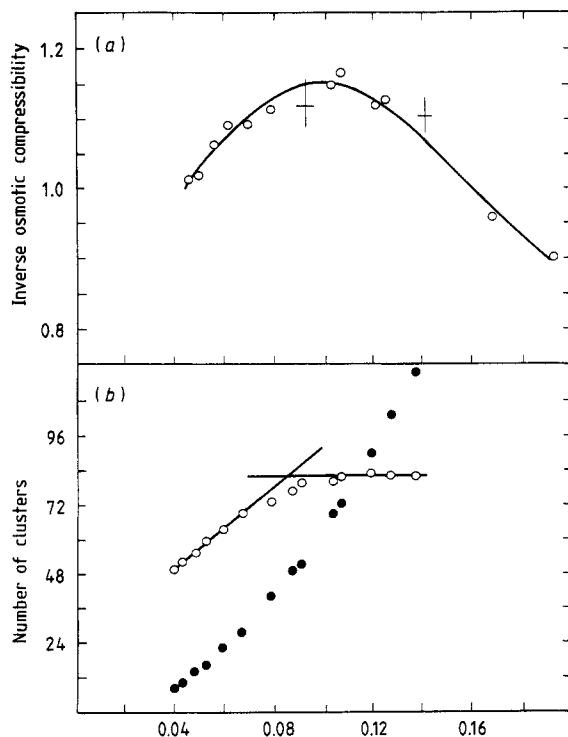


**Figure 2.** The variation of (a) the inverse osmotic compressibility  $\partial\pi/\partial n_s$  and of (b) the number of small (open circles) and large (full circles) micelles with the surfactant concentration  $n_s$ . The CMC can be estimated from the position of the maximum of the curve (a); the intersection point (shown for small clusters) of the asymptotes to the two far ends of the curves (b) also gives an estimate for the CMC. Parameter values are as in figure 1, with  $T = 0.22J$ .

individual couplings and obtain simultaneously a conventional coexistence curve in the oil–surfactant limit with an upper consolute point at  $T = T_\beta$ . Furthermore, we can have  $T_\alpha > T_\beta$ . Such a situation occurs in many oil–water–surfactant mixtures. Then, following the arguments of Kahlweit, Lessner and Strey [10], we can conclude that a system with  $T_\alpha > T_\beta$  can exhibit three-phase coexistence between oil-rich, water-rich, and microemulsion phases. The details of the oil–surfactant limit and of such three-phase coexistence in our model (1) will be given elsewhere [11].

To summarise, we have given a lattice model of oil–water–surfactant mixtures that has qualitatively correct behaviour in the water–surfactant and oil–surfactant limits when compared to many real systems. One may therefore expect that its behaviour in general will reflect many of the properties of systems showing microemulsion phases.

We would like to thank K Chen for extremely useful discussions. One of us (RP) would like to thank the University Grants Commission and the Department of Science and Technology (India) for support and the Department of Physics, Ohio State University, for hospitality while some of this work was being done. Support from NSF Grants no DMR-8451922 and DMR-8705606 is gratefully acknowledged. We also thank the Ohio

Supercomputer Center for use of the CRAY X-MP on which the simulations were performed.

## References

- [1] Mittal K L and Lindman B (ed.) 1986 *Surfactants in Solution* vol 1–4 (New York: Plenum)  
Mittal K L (ed.) 1977 *Micellization, Solubilization, and Microemulsions* vol 1 and 2 (New York: Plenum)  
Degiorgio V and Corti M (ed.) 1985 *Physics of Amphiphiles: Micelles, Vesicles, and Microemulsions* (New York: Academic)
- [2] Meguro K, Ueno M and Esumi K 1987 *Non-Ionic Surfactants-Physical Chemistry* vol. 23 ed. M Schick (New York: Dekker)
- [3] Lang J C and Morgan R D 1980 *J. Chem. Phys.* **73** 5849
- [4] Chen K, Ebner C, Jayaprakash C and Pandit R 1988 *Phys. Rev. A* **38** 6240  
Halley J W and Kolan A J 1988 *J. Chem. Phys.* **88** 3313
- [5] Anderson G R and Wheeler J C 1978 *J. Chem. Phys.* **69** 1082  
Walker J S and Vause C A 1982 *Phys. Lett. A* **90** 419  
Goldstein R E and Walker J S 1983 *J. Chem. Phys.* **78** 1492
- [6] Stillinger F H and Ben-Naim A 1981 *J. Chem. Phys.* **74** 2510  
Goldstein R E 1986 *J. Chem. Phys.* **84** 3367
- [7] Blankschtein D, Thurston G M and Benedek G 1986 *J. Chem. Phys.* **85** 7268
- [8] Elworthy P H, Florence A T and Macfarlane C B 1968 *Solubilization by Surface-Active Agents* (London: Chapman)
- [9] Prigogine I 1957 *The Molecular Theory of Solutions* (Amsterdam: North Holland) pp 88–98  
Kirkwood J G 1968 *Theory of Solutions* (New York: Gordon and Breach) pp 82–89
- [10] Kahlweit M, Lessner E and Strey R 1983 *J. Phys. Chem.* **87** 5032
- [11] Wenzel W, Ebner C, Jayaprakash C and Pandit R 1989 unpublished